Textile Dye Removal from Single and Ternary Systems Using Date Stones: Kinetic, Isotherm, and Thermodynamic Studies

Niyaz Mohammad Mahmoodi,[†] Bagher Hayati,[‡] and Mokhtar Arami*[,‡]

Department of Environmental Research, Institute for Color Science and Technology, Tehran, Iran, and Textile Engineering Department, Amirkabir University of Technology, Tehran, Iran

In this paper, the removal of the dyes acid green 25 (AG25), acid black 26 (AB26), and acid blue 7 (AB7) onto date stones (DS) from single and ternary systems was investigated. Surface studies of DS were investigated by Fourier transform infrared (FTIR) and scanning electron microscopy (SEM). Experiments were carried out as a function of adsorbent dosage, initial dye concentration, inorganic anion (salt), pH, and temperature in single and ternary systems. The adsorption kinetics, isotherms, thermodynamics, and dye desorption were studied in single and ternary dye systems. The adsorption kinetics was modeled using the pseudofirst-order, pseudosecond-order, and intraparticle diffusion kinetics equations. The equilibrium adsorption data of AG25, AB26, and AB7 dyes on DS were analyzed. Thermodynamic parameters of dye adsorption were obtained. In addition, the regeneration of DS was studied using dye desorption in single and ternary dye systems. The adsorption kinetics of the dyes followed pseudosecond-order kinetics. The results indicate that the Langmuir model provides the best correlation of the experimental data. The thermodynamic studies showed that the dye adsorption onto DS was a spontaneous, endothermic, and physical reaction. A high desorption of AG25, AB26, and AB7 showed the regeneration of DS. It can be concluded that DS are suitable as an adsorbent material to remove AG25, AB26, and AB7 dyes from single and ternary systems.

Introduction

The textile dyeing industry consumes large quantities of water at its different steps of dyeing and finishing, among other processes. The nonbiodegradable nature of dyes and their stability toward light and oxidizing agents complicate the selection of a suitable method for their removal. Moreover, toxicity bioassays have demonstrated that most dyes are toxic.[1−6]

Dyes may drastically affect photosynthetic phenomena in aquatic life because of reduced light penetration.[7,8] As a result, the removal of color from waste effluents has become environmentally important.[9,10] Various methods, including coagulation,[11] chemical oxidation,[12] adsorption,[13,14] electrochemistry,[15] and so forth, have been examined. Among the above-mentioned methods, adsorption is considered to be superior to other techniques because of low cost, the simplicity of design, availability, and the ability to treat dyes in a more concentrated form.[16,17] Activated carbon has been widely studied and proven to have high adsorption abilities to remove a large number of organic compounds. However, its use is limited mainly because of its high cost.[18,19] So, the research of recent years mainly focused on utilizing natural materials as alternatives to activated carbon.[18−20] Several adsorbents have been used already.[16−23]

A literature review showed that date stones (DS) have not been used to remove dyes from colored wastewater. The world production of dates was approximately 6.7 million tonnes in 2004. The major producers in the world are Egypt, Iran, Saudi Arabia, United Arab Emirates, Pakistan, Algeria, and other Mediterranean countries. Algeria produces 450 000 tonnes per year of dates.[24,25] In this research, DS were used as an adsorbent to remove three acid dyes from aqueous solution in single and ternary systems. Acid green 25 (AG25), acid black 26 (AB26), and acid blue 7 (AB7) were used as model dyes. Acid dyes denote a large group of anionic dyes with a relatively low molecular weight that carry one to three sulfonic groups. They are mainly monoazo compounds but also include diazo, nitro, 1-amino-anthraquinone, triphenyl methane, and other groups of compounds. The name "acid dye" is derived from the dyeing process; the dyes are applied to wool, silk, and polyamides in weakly acid solution (pH 2 to 6).[26] Effective parameters such as adsorbent dosage, dye concentration, inorganic anions (salt), pH, and temperature were investigated for dye removal. Kinetics, isotherm, and thermodynamic studies were conducted to evaluate the adsorption capacity of DS in single and ternary systems.

Experimental Section

Chemicals and Materials. DS were obtained from a local fruit field in Iran. The DS were washed to remove the adhering dirt and then dried, crushed, and sieved. They were dried at room temperature (25 °C) for 24 h. After drying, they were sieved through a 3.36 mm mesh. The acid dyes (AG25, AB26, and AB7) were used. The dyes were purchased from Ciba Ltd. The chemical structure of the dyes is shown in Figure 1. Other chemicals were Analar grade from Merck. The Fourier transform infrared (FTIR) spectrum of DS was prepared with a Perkin-Elmer spectrophotometer Spectrum One in the range of (450 to 4000) cm^{-1}. A CECIL 2021 UV−vis spectrophotometer was used to determine the dye removal. Scanning electron microscopy (SEM) studies were performed using Philips XL30 images.

* Corresponding author. Tel.: +98 21 64542614; Fax: +98 21 66400245. E-mail address: arami@aut.ac.ir (M. Arami).
[†] Institute for Color Science and Technology. E-mail: nm_mahmoodi@aut.ac.ir (N. M. Mahmoodi).
[‡] Amirkabir University of Technology.

10.1021/je1002384
Published on Web 10/15/2010

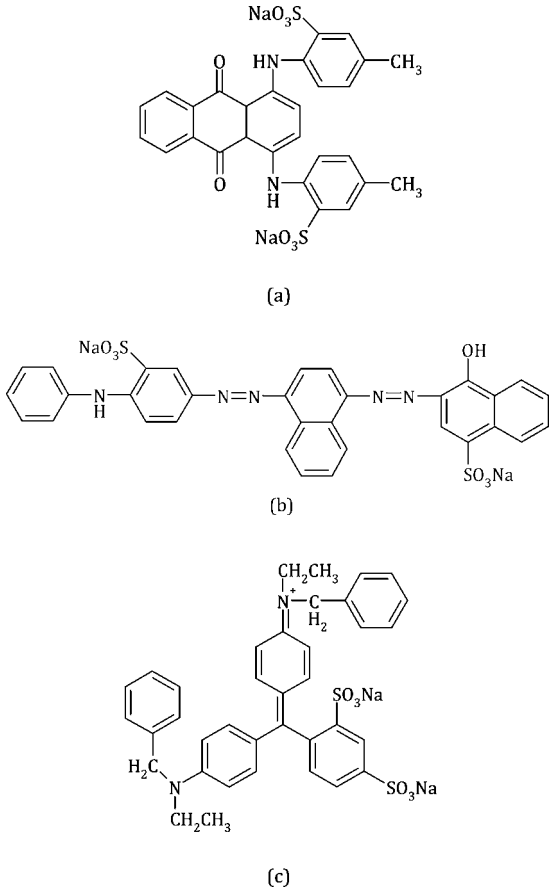

Figure 1. Chemical structure of the dyes (a) AB26, (b) AB7, and (c) AG25.

Adsorption Tests. The adsorption measurements were conducted using various amounts of DS [(1 to 2) $g \cdot L^{-1}$] for AB26, AG25, and AB7 in jars containing 200 mL of a dye solution (50 $mg \cdot L$) at various pH values (2 to 12). The pH of the solution was adjusted by adding a small amount of H_2SO_4 or NaOH. Dye solutions were prepared using distilled water to prevent and minimize possible interferences. Adsorption experiments were performed at various concentrations of dye solutions using the optimum amount of DS (DS = 2 $g \cdot L^{-1}$ for AB26, AG25, and AB7) at pH 2 and 25 °C for 40 min to attain the equilibrium conditions. The absorbance of all samples were monitored and determined at certain time intervals [(2.5, 5, 10, 15, 20, 25, 30, 35, and 40) min] during the adsorption process. After the experiments, the samples were centrifuged by a Hettich EBA20, and then the dye concentration was determined. To investigate inorganic ion (salts) effects on dye removal efficiency, 1 mmol of Na_2SO_4, $NaHCO_3$, K_2CO_3, and NaCl were added to the dye solution (200 mL). The equilibrium was established after 30 min. At the end of the adsorption experiments, the samples were centrifuged, and the dye concentration was determined. For thermodynamic studies, the adsorption of dyes at different temperatures [(25 to 65) °C] was performed.

Dye concentrations were calculated as follows: for a ternary system of components *A*, *B*, and *C* that were measured at wavelengths of λ_1, λ_2, and λ_3, respectively, to give optical densities of d_1, d_2, and d_3:

$$C_A = (d_1X + d_2Y + d_3Z)/(k_{A1}X + k_{A2}Y + k_{A3}Z) \quad (1)$$

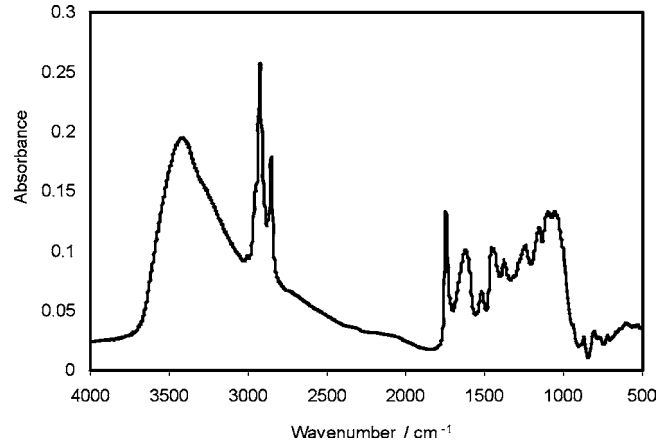

Figure 2. FTIR spectrum of DS.

$$(X = k_{B3}k_{C2} - k_{B2}k_{C3}; \quad Y = k_{B1}k_{C3} - k_{B3}k_{C1}; \quad Z = k_{B2}k_{C1} - k_{B1}k_{C2})$$

$$C_B = (d_1X' + d_2Y' + d_3Z')/(k_{B1}X' + k_{B2}Y' + k_{B3}Z') \quad (2)$$

$$(X' = k_{A2}k_{C3} - k_{A2}k_{C2}; \quad Y' = k_{A3}k_{C1} - k_{A1}k_{C3}; \quad Z' = k_{A1}k_{C2} - k_{A2}k_{C1})$$

$$C_C = (d_1X'' + d_2Y'' + d_3Z'')/(k_{B1}X'' + k_{B2}Y'' + k_{B3}Z'') \quad (3)$$

$$(X'' = k_{A2}k_{B3} - k_{A3}k_{B2}; \quad Y'' = k_{A3}k_{B1} - k_{A1}k_{B3}; \quad Z'' = k_{A1}k_{B2} - k_{A2}k_{B1})$$

where k_{A1}, k_{B1}, k_{C1}, k_{A2}, k_{B2}, k_{C2}, k_{A3}, k_{B3}, and k_{C3} are the calibration constants for components *A*, *B*, and *C* at the three wavelengths λ_1, λ_2, and λ_3, respectively.

Surface Studies. The FTIR spectrum of DS was prepared with a Perkin-Elmer spectrophotometer. The surface images of DS before and after the adsorption process were captured by SEM. The experiments were conducted with 200 mL dye solutions (AB26, AG25, and AB7) with a concentration of 50 $mg \cdot L^{-1}$ at pH 2 and 2 $g \cdot L^{-1}$ DS. DS powders were separated from the solutions and dried for 120 min at 50 °C. Then the DS samples were visually examined by SEM.

Desorption Studies. The biosorbent that was used for the adsorption of dye solution was separated from solution by filtration and then were dried. It was agitated with 200 mL of distilled water at different pH values (2 to 12) for the predetermined equilibrium time of the adsorption process. The desorbed dye was measured.

Results and Discussion

Surface Characteristics. The FTIR spectrum of DS (Figure 2) shows that the peak positions are at (3422.70, 2923.24, 2851.89, 1742.70, 1619.46, and 1061.62) cm^{-1}. The band at 3422.70 cm^{-1} is due to O—H and N—H stretching, while the bands at (1742.70, 1619.46, and 1450.81) cm^{-1} reflect the carbonyl group stretching, C═C stretching, and N—H bending, respectively. The band at 1061.62 cm^{-1} corresponds to C—O stretching.[27]

SEM has been a primary tool for characterizing the surface morphology and fundamental physical properties of adsorbent

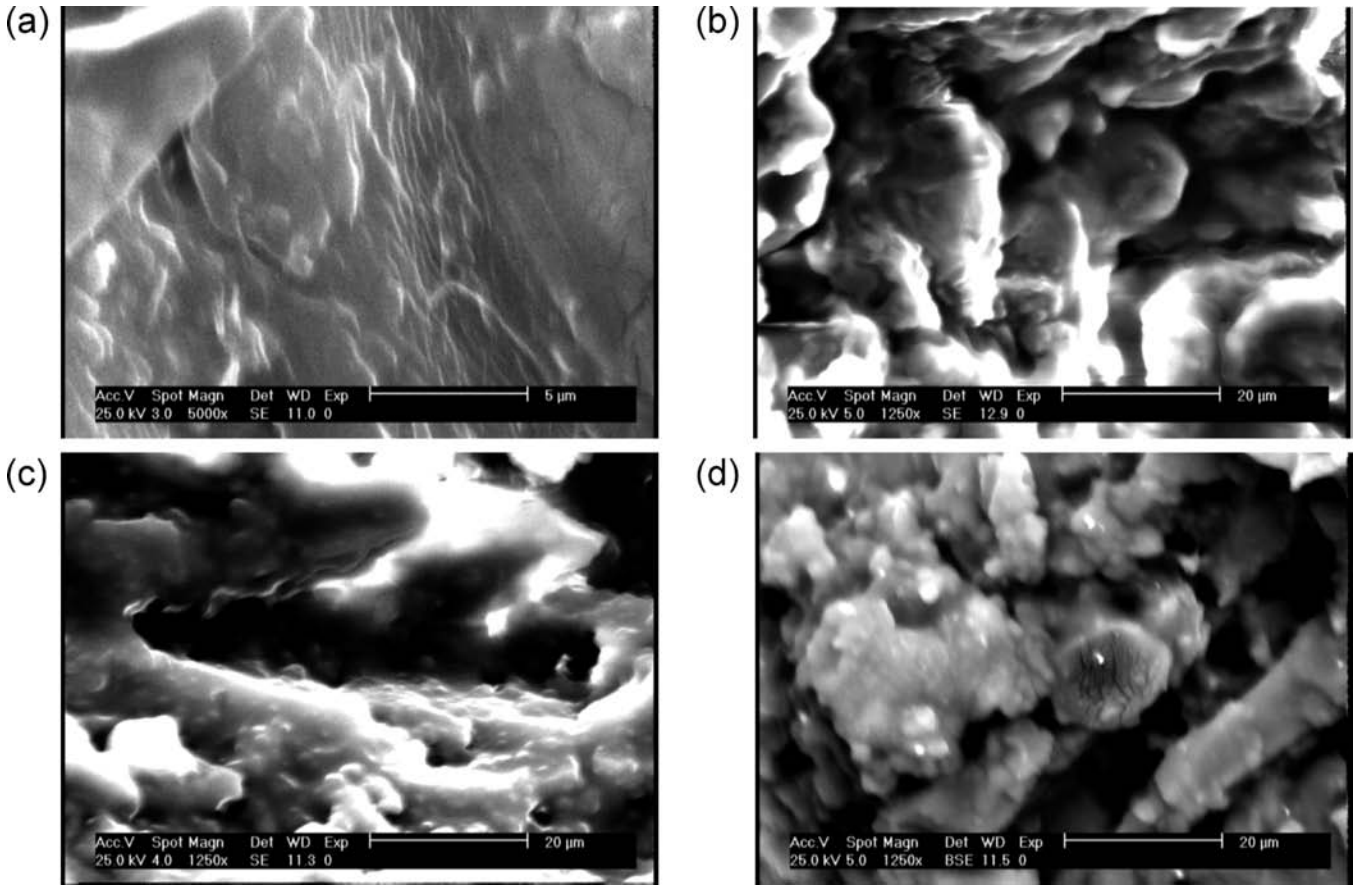

Figure 3. SEM images of raw and dye adsorbed DS after 30 min. (a) Raw DS, (b) dye adsorbed DS (AG25), (c) dye adsorbed DS (AB26), and (d) dye adsorbed DS (AB7).

surfaces. It is useful for determining the particle shape, porosity, and appropriate size distribution of the adsorbent. Scanning electron micrographs of raw DS and adsorbed DS with AG25, AB26, and AB7 are shown in Figure 3. From Figure 3, it is clear that DS has considerable numbers of pores where there is a good possibility for dyes to be trapped and adsorbed into these pores. The SEM pictures of the DS samples show very distinguished dark spots which can be taken as a sign for the effective adsorption of dye molecules in the cavities and pores of this adsorbent.

Effective Parameters on Dye Removal. Adsorbent Dosage Effect. The effect of DS dosages on dye removal in single and ternary systems was investigated by contacting 200 mL of dye solution with an initial dye concentration of 50 $mg \cdot L^{-1}$ using jar tests at room temperature (25 °C) for 30 min. Different amounts of DS [(1 to 3) $g \cdot L^{-1}$] for AB26, AG25, and AB7 were applied. After equilibrium, the samples were centrifuged, and the concentration in the supernatant dye solution was analyzed. A plot of dye removal (%) versus time at different adsorbent dosage is shown in Figure 4.

The increase in adsorption with adsorbent dosage can be attributed to an increased adsorbent surface and the availability of more adsorption sites. However, if the adsorption capacity is expressed in milligrams adsorbed per gram of material, the capacity decreases with the increasing amount of sorbent. This may be attributed to overlapping or aggregation of adsorption sites, resulting in a decrease in total adsorbent surface area available to the dye and an increase in diffusion path length.[13]

Dye Concentration Effect. The effects of initial dye concentration on dye removal in single and ternary systems were studied. Experiments were conducted at different dye concentrations of (25, 50, 75, and 100) $mg \cdot L^{-1}$ [(DS: 2 $g \cdot L^{-1}$ for AB26, AG25, and AB7), pH 2, and 200 mL dye solution]. For all dyes, the equilibrium capacity decreases with an increase in the initial concentrations as shown in Figure 5. It can be attributed that the active sites on the adsorbent for dye removal decrease when the dye concentration increases.

The amount of the dye adsorbed onto DS increases with an increase in the initial dye concentration at a constant amount of adsorbent. This is due to the increase in the driving force of the concentration gradient with the higher initial dye concentrations. At low initial dye concentrations, the adsorption of dyes by DS is very intense and reaches equilibrium very quickly. This indicates the possibility of the formation of monolayer coverage of the molecules at the outer interface of the DS. At a fixed DS dosage, the residual concentration of dye molecules will be higher for higher initial dye concentrations. In the case of lower dye concentrations, the ratio of initial number of dye moles to the available adsorption sites is low. At higher concentrations, the number of available adsorption sites becomes lower, and subsequently the removal of dyes depends on the initial concentration. At high concentrations, it is not likely that dyes are only adsorbed in a monolayer at the outer interface of biosorbent.[6,14,28,29]

Inorganic Anion (Salt) Effect. The occurrence of dissolved inorganic ions is rather common in dye-containing industrial wastewater.[5] These substances may compete for the active sites on the adsorbent surface and, subsequently, decrease the dye removal efficiency. A major drawback resulting from the reactivity and nonselectivity of active sites on the adsorbent is that it also reacts with nontarget compounds present in the background water matrix, that is, dye auxiliaries present in the

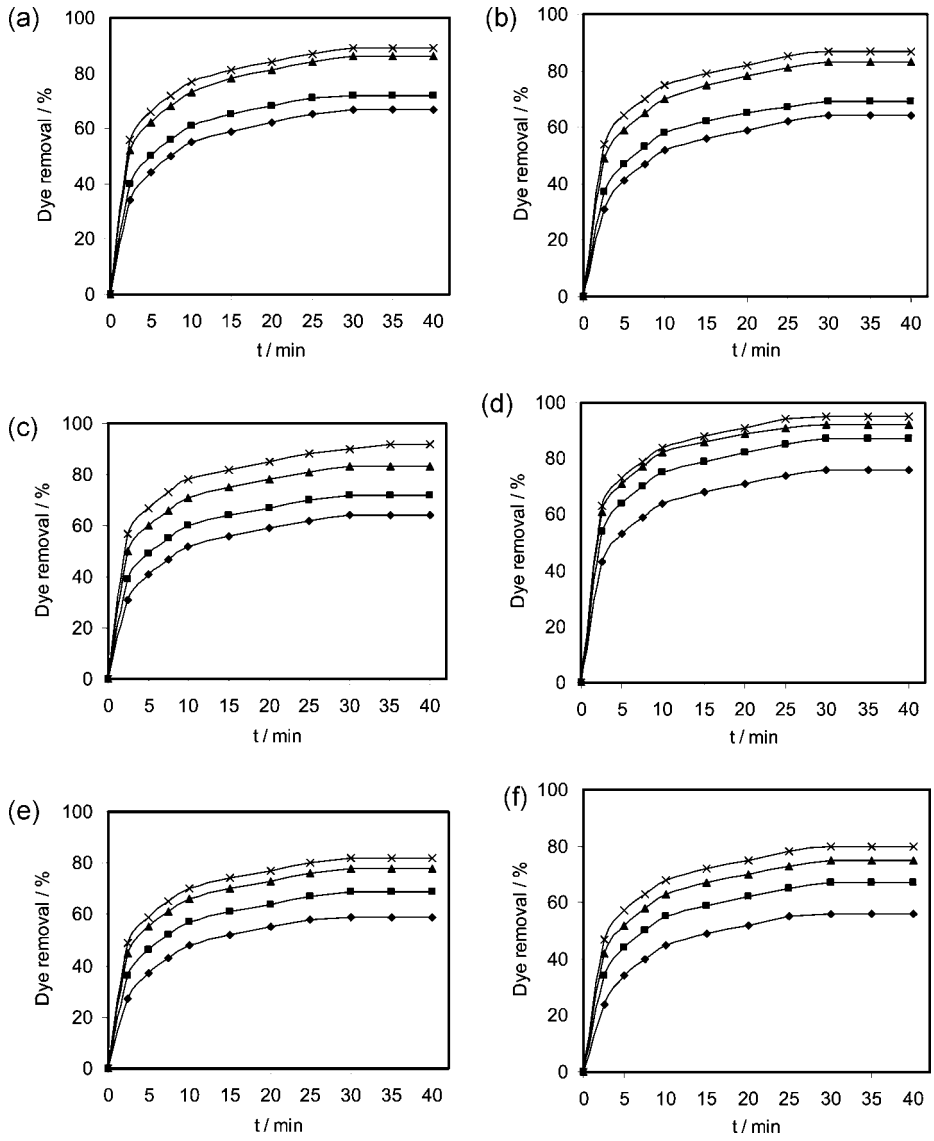

Figure 4. Effect of adsorbent dosage on dye removal by DS in single (sin) and ternary (ter) systems: (a) AG25 (sin), (b) AG25 (ter), (c) AB26 (sin), (d) AB26 (ter), (e) AB7 (sin), and (f) AB7 (ter) (C_0 = 50 mg·L^{-1}, pH 2, and 25 °C). Adsorbent/g·L^{-1}: ◆, 1; ■, 1.5; ▲, 2; and ×, 3.

exhausted dye bath. This results in a higher adsorbent demand to accomplish the desired degree of dye removal.

To investigate the effect of inorganic anions on dye removal in single and ternary systems, Na_2SO_4, $NaHCO_3$, K_2CO_3 and NaCl were added to the dye solution. Figure 6 illustrates that the dye removal capacity of dyes by DS decreases in the presence of inorganic salts because these salts have small molecules and compete with dyes for adsorption onto DS.

pH Effect. The results of blank dye solution studies indicated that a change of the initial pH of the dye solution has a negligible effect on the λ_{max} of AB26, AG25, and AB7 dyes (pH 2 to 12), and during the experiments the pH of the dye solutions was not changed significantly. This observation proved that, over this range of pH, no chemical structural change of the dye molecules occurs. On the basis of this observation and assuming negligible dissociation of the adsorbent, the pH of all dye solutions was reported as the initial pH, and pH control during all experiments was ignored. The maximum absorbance wavelength (λ_{max}) of AB26, AG25, and AB7 at different pH values is shown in Table 1.

The effect of the initial pH on the dye removal in single and ternary systems is shown in Figure 7. The adsorption capacity increases when the pH decreases. Maximum adsorption of acid dyes occurs at an acidic pH (pH 2). DS are comprised of various functional groups, such as amino, hydroxyl, and carbonyl groups which are affected by the pH of solutions. Therefore, at various pH values, electrostatic attraction as well as the ionic properties and structure of dye molecules and DS could play very important roles in the dye adsorption on DS. At pH 2, a considerably high electrostatic attraction exists between the positively charged surface of the adsorbent, due to the ionization of functional groups of the adsorbent and negatively charged anionic dye molecules. As the pH of the system increases, the number of negatively charged sites increases. A negatively charged site on the adsorbent does not favor the adsorption of anionic dyes due to electrostatic repulsion.[30] Also, a lower adsorption of AB26, AG25, and AB7 dyes at the alkaline pH is due to the presence of excess OH^- ions destabilizing anionic dyes and competing with the dye anions for the adsorption sites. Thus, the effective pH was 2, and it was used in further studies.

Temperature Effect. The adsorption studies in single and ternary systems were carried out at different temperatures [(25, 35, 45, 55, and 65) °C], and the results of these experiments are shown in Figure 8. The adsorption capacity increases with the increasing temperature,

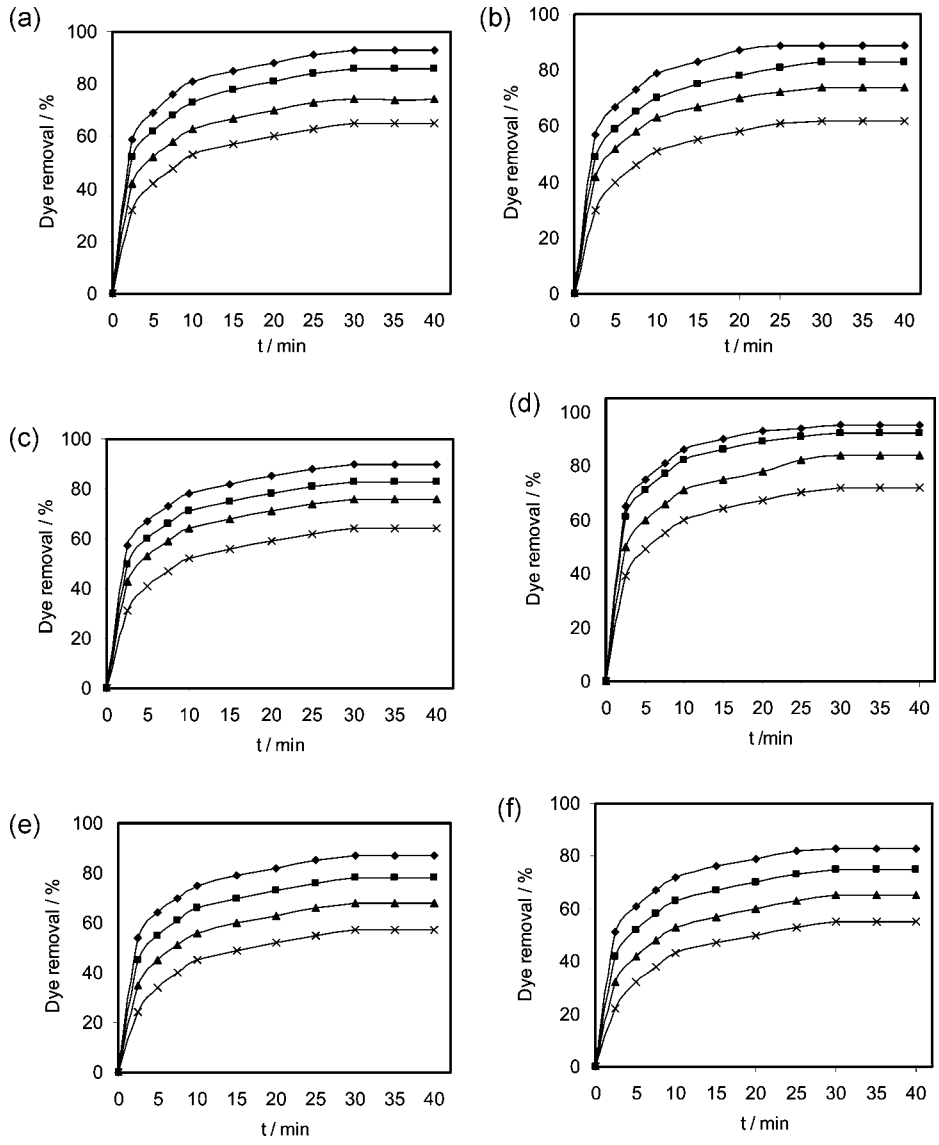

Figure 5. Effect of dye concentration on dye removal by DS in single (sin) and ternary (ter) systems: (a) AG25 (sin), (b) AG25 (ter), (c) AB26 (sin), (d) AB26 (ter), (e) AB7 (sin), and (f) AB7 (ter) (pH 2, 25 °C, and DS = 2 g·L^{-1} for AG25, AB26, and AB7). Dye/mg·L^{-1}: ◆, 25; ■, 50; ▲, 75; and ×, 100.

indicating that the adsorption is an endothermic process. This may be a result of an increase in the mobility of the dye with increasing temperature.[31] An increasing number of molecules may also acquire sufficient energy to undergo an interaction with active sites at the surface. Furthermore, the increasing temperature may produce a swelling effect within the internal structure of the DS, enabling the large dye to penetrate further.[32]

Adsorption Kinetics. Several models can be used to express the mechanism of solute sorption onto a sorbent. To design a fast and effective model, investigations were made on the adsorption rate. For the examination of the controlling mechanisms of the adsorption process, such as chemical reaction, diffusion control and mass transfer, several kinetics models are used to test the experimental data.[33,34]

The pseudofirst-order equation is generally represented as follows:[35,36]

$$dq_t/dt = k_1(q_e - q_t) \quad (4)$$

where q_e, q_t, and k_1 are the amount of dye adsorbed at equilibrium (mg·g^{-1}), the amount of dye adsorbed at time t (mg·g^{-1}), and the equilibrium rate constant of pseudofirst order kinetics (min^{-1}), respectively. After integration and applying conditions, $q_t = 0$ at $t = 0$ and $q_t = q_t$ at $t = t$, then eq 4 becomes

$$\log(q_e - q_t) = \log(q_e) - (k_1/2.303)t \quad (5)$$

The straight-line plots of $\log(q_e - q_t)$ versus t for the adsorption of AB26, AG25, and AB7 onto DS at different dye concentrations [(25, 50, 75, and 100) mg·L^{-1}] have also been tested to obtain the rate parameters. The k_1, the calculated q_e ($(q_e)_{Cal}$), and the coefficient of determination (R^2) were calculated and are given in Table 2 for single and ternary systems.

Data were applied to the pseudosecond-order kinetic rate equation which is expressed as:[35,37]

$$dq_t/dt = k_2(q_e - q_t) \quad (6)$$

where k_2 is the equilibrium rate constant of the pseudosecond-order kinetic model (g·mg^{-1}·min^{-1}). On integrating eq 6,

$$t/q_t = 1/k_2q_e^2 + (1/q_e)t \quad (7)$$

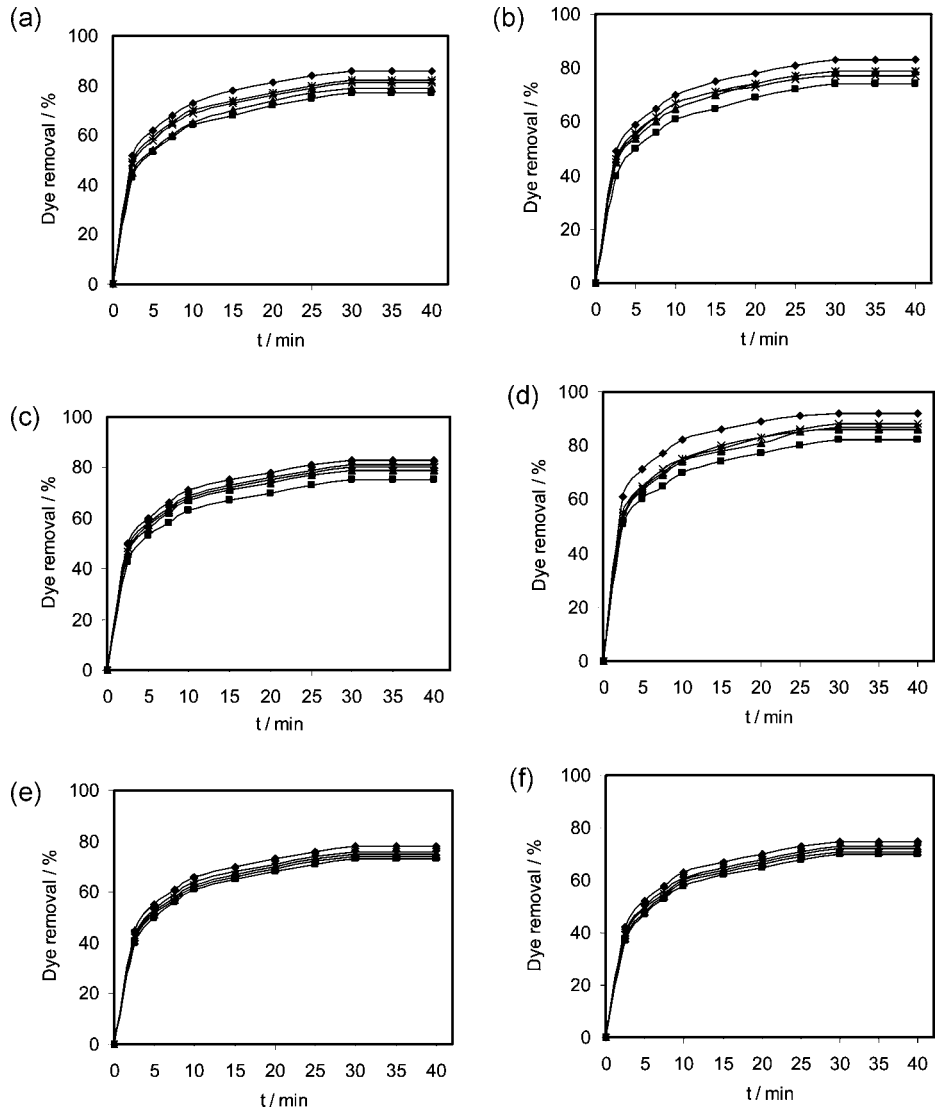

Figure 6. Effect of inorganic ions on dye removal by DS in single (sin) and ternary (ter) systems: (a) AG25 (sin), (b) AG25 (ter), (c) AB26 (sin), (d) AB26 (ter), (e) AB7 (sin), and (f) AB7 (ter) (C_0 = 50 mg·L^{-1}, pH 2, 25 °C, and DS = 2 g·L^{-1} for AG25, AB26, and AB7). Salt: ◆, no salt; ■, NaCl; ▲, Na_2SO_4; ×, $NaHCO_3$; and ∗, K_2CO_3.

Table 1. Effect of the Initial pH of Dye Solutions on the Maximum Absorbance Wavelength (λ_{max} (nm)) of AB26, AG25, and AB7

	λ_{max} (nm)		
pH	AB26	AG25	AB7
2	550	605	640
4	552	603	638
6	551	602	641
8	550	604	639
10	549	605	641
12	552	603	641

To understand the applicability of the model, linear plots of t/q_t versus t under dye concentration values [(25, 50, 75, and 100) mg·L^{-1}] for the adsorption of AB26, AB7, and AG25 onto DS were plotted. The k_2, the calculated q_e ($(q_e)_{Cal}$), and the coefficient of determination (R^2) were calculated and are given in Table 2 for single and ternary systems.

The possibility of intraparticle diffusion resistance affecting adsorption was explored by using the intraparticle diffusion model as

$$q_t = k_p t^{1/2} + 1 \quad (8)$$

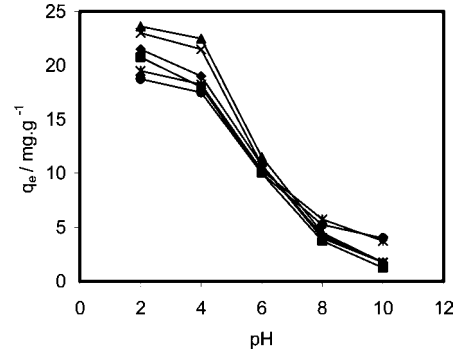

Figure 7. Effect of pH on the adsorption of dyes onto DS in single and ternary systems (C_0 = 50 mg·L^{-1}, 25 °C, and DS = 2 g·L^{-1} for AG25, AB26, and AB7). ◆, AG25 (sin); ■, AG25 (ter); ▲, AB26 (sin); ×, AB26 (ter); ∗ AB7 (sin), and ●, AB7 (ter).

where k_p is the intraparticle diffusion rate constant (mg·g^{-1}·min$^{-1/2}$).

Values of I (Table 2 for single and ternary systems) give an idea about the thickness of the boundary layer, that is, the larger the intercept, the greater the boundary layer effect is. According to this model, a plot of uptake should be linear if intraparticle

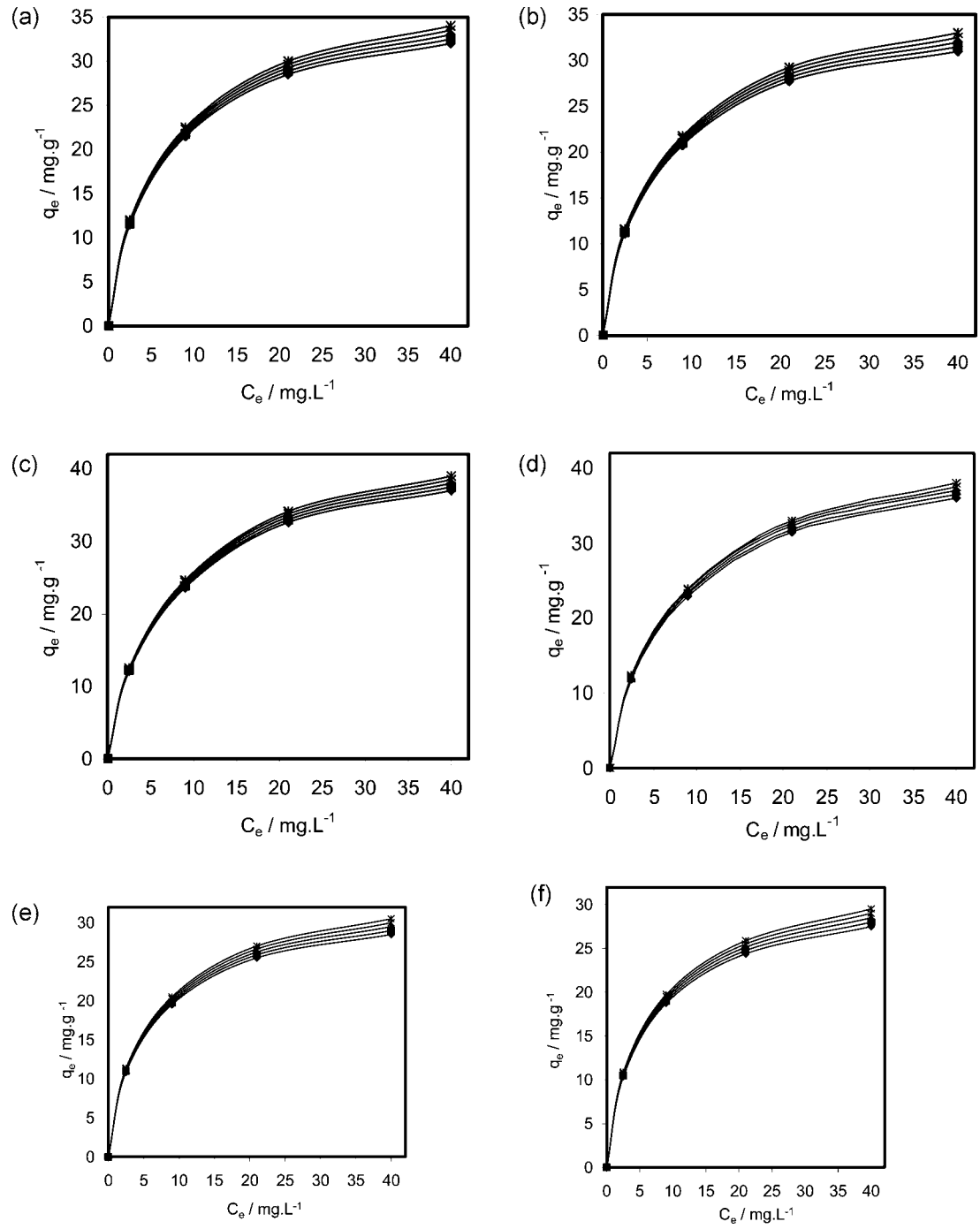

Figure 8. Adsorption of dyes onto DS at different temperatures (°C) in single (sin) and ternary (ter) systems (a) AG25 (sin), (b) AG25 (ter), (c) AB26 (sin), (d) AB26 (ter), (e) AB7 (sin), and (f) AB7 (ter) (C_0 = 50 mg·L^{-1}, pH 2, and DS = 2 g·L^{-1} for AG25, AB26, and AB7). t/°C: ◆, 25; ■, 35; ▲, 45; ×, 55; and ∗, 65.

diffusion is involved in the adsorption process, and if these lines pass through the origin, then intraparticle diffusion is the rate-controlling step.[38−40] When the plots do not pass through the origin, this indicates some degree of boundary layer control and shows that the intraparticle diffusion is not the only rate-limiting step, but also other kinetic models may control the rate of adsorption, all of which may be operating simultaneously.

The linear fit between the t/q_t versus contact time (t) and calculated coefficient of determination (R^2) for the pseudosecond-order kinetics model shows that the dye removal kinetics can be approximated as a pseudosecond order kinetics model (Table 2). In addition, the experimental q_e ($(q_e)_{Exp}$) values agree with the calculated ones ($(q_e)_{Cal}$), obtained from the linear plots of the pseudosecond-order kinetics model (Table 2).

Adsorption Isotherms. To optimize the design of an adsorption system for the adsorption of adsorbates, it is important to establish the most appropriate correlation for the equilibrium curves. Various isotherm equations like those of Langmuir, Freundlich, and Tempkin for single systems and the extended Langmuir, extended Freundlich, and Tempkin isotherms for ternary systems were tested in this work.

In the Langmuir theory, the basic assumption is that the sorption takes place at specific homogeneous sites within the adsorbent. This equation can be written as follows:[41−46]

$$q_e = Q_0 K_L C_e/(1 + K_L C_e) \quad (9)$$

Table 2. Kinetics Constants for Dye Adsorption by DS at (25, 50, 75, and 100) mg·L^{-1} Dye Concentrations in Single and Ternary Systems (200 mL Solution, pH 2.5, 25 °C, and DS = 2 g·L^{-1} for AG25, AB26, and AB7) (Dye/mg·L^{-1}; $(q_e)_{Exp}$/mg·g^{-1}; $(q_e)_{Cal}$/mg·g^{-1}; k_1/min^{-1}; k_2/g·mg^{-1}·min^{-1}; and K_p/mg·g^{-1}·min$^{-1/2}$)

			pseudofirst order			pseudosecond order			intraparticle diffusion		
	dye	$(q_e)_{Exp}$	$(q_e)_{Cal}$	k_1	R^2	$(q_e)_{Cal}$	k_2	R^2	K_p	I	R^2
Single System						AG25					
	25	11.625	7.040	0.133	0.954	12.050	0.054	0.998	1.506	3.824	0.756
	50	21.500	13.920	0.131	0.964	22.420	0.026	0.998	2.855	6.596	0.787
	75	27.940	19.850	0.137	0.969	29.240	0.018	0.997	3.797	8.013	0.808
	100	32.500	24.430	0.125	0.977	34.600	0.011	0.995	4.642	7.791	0.859
						AB26					
	25	12.125	7.081	0.167	0.970	12.469	0.076	0.999	1.506	4.518	0.693
	50	23.625	15.922	0.181	0.965	24.331	0.036	0.999	2.971	8.566	0.708
	75	32.250	20.123	0.131	0.957	33.557	0.018	0.998	4.234	10.213	0.773
	100	37.000	25.509	0.127	0.968	38.580	0.013	0.997	5.072	10.288	0.820
						AB7					
	25	10.875	6.720	0.129	0.952	11.290	0.054	0.998	1.423	3.473	0.770
	50	19.500	13.030	0.128	0.965	20.370	0.026	0.997	2.631	5.699	0.804
	75	25.500	18.580	0.125	0.973	26.950	0.016	0.996	3.589	6.467	0.846
	100	28.500	23.320	0.122	0.984	30.770	0.010	0.993	4.260	5.571	0.893
Ternary System						AG25					
	25	11.125	6.711	0.148	0.949	11.534	0.064	0.998	1.446	3.754	0.744
	50	20.750	13.804	0.131	0.967	21.692	0.025	0.997	2.784	6.179	0.798
	75	27.750	18.493	0.133	0.971	28.985	0.018	0.997	3.763	8.070	0.803
	100	31.000	25.972	0.146	0.972	33.003	0.012	0.995	4.461	7.415	0.855
						AB26					
	25	11.875	7.031	0.166	0.972	12.210	0.075	0.999	1.482	4.379	0.698
	50	23.000	14.342	0.159	0.969	23.753	0.034	0.999	2.920	8.105	0.723
	75	31.500	20.649	0.127	0.952	32.895	0.016	0.997	4.203	9.442	0.796
	100	36.000	25.275	0.127	0.970	37.879	0.012	0.996	4.976	9.733	0.829
						AB7					
	25	10.375	7.163	0.152	0.962	10787	0.059	0.998	1.366	3.310	0.769
	50	18.750	12.814	0.128	0.967	19.646	0.026	0.997	2.560	5.283	0.816
	75	24.375	18.315	0.125	0.976	25.840	0.015	0.995	3.481	5.843	0.859
	100	27.500	23.089	0.121	0.985	29.851	0.010	0.992	4.164	5.017	0.902

Table 3. Isotherm Constants for Dye Adsorption by DS at Different Temperatures in Single System (200 mL Solution, pH 2, C_0 = 50 mg·L^{-1}, and DS = 2 g·L^{-1} for AG25, AB26, and AB7) (Q_0/mg·g^{-1}; K_L/L·mg^{-1}; K_F/L·g^{-1}; K_T/mg·L^{-1}; and B_1/mg·g^{-1})

	Langmuir isotherm model				Freundlich isotherm model			Tempkin isotherm model		
temperature/°C	Q_0	K_L	R_L	R^2	K_F	n	R^2	K_T	B_1	R^2
					AG25					
25	35.842	0.223	0.082	0.999	9.638	2.793	0.959	2.628	7.198	0.993
35	36.101	0.247	0.075	0.999	10.256	2.882	0.962	3.124	7.068	0.995
45	36.232	0.279	0.067	0.999	10.940	2.817	0.966	3.824	6.902	0.996
55	36.496	0.317	0.059	0.999	11.722	3.115	0.970	4.869	6.692	0.997
65	36.496	0.369	0.051	0.998	12.647	3.279	0.975	6.562	6.425	0.998
					AB26					
25	39.526	0.543	0.035	0.999	14.863	3.196	0.931	8.576	7.081	0.984
35	39.370	0.715	0.027	0.999	16.520	3.499	0.943	14.789	6.524	0.989
45	39.216	1.024	0.019	0.999	18.810	4.031	0.964	37.061	5.691	0.997
55	39.062	1.730	0.011	0.998	21.355	4.771	0.979	89.962	5.109	0.998
65	39.370	2.288	0.009	0.998	22.336	4.840	0.944	115.367	5.106	0.983
					AB7					
25	33.113	0.140	0.125	0.999	7.283	2.627	0.975	1.499	6.950	0.997
35	33.445	0.150	0.118	0.999	7.631	2.668	0.977	1.648	6.939	0.997
45	33.784	0.160	0.111	0.999	8.011	2.716	0.979	1.831	6.912	0.998
55	34.130	0.172	0.104	0.998	8.429	2.772	0.981	2.059	6.867	0.998
65	34.483	0.186	0.097	0.998	8.890	2.836	0.982	2.349	6.800	0.998

where C_e, K_L, and Q_0 are the equilibrium concentrations of dye solution (mg·L^{-1}), the Langmuir constant (L·mg^{-1}), and the maximum adsorption capacity (mg·g^{-1}), respectively.

The linear form of the Langmuir equation is:

$$C_e/q_e = 1/K_L Q_0 + C_e/Q_0 \quad (10)$$

The essential characteristic of the Langmuir isotherm can be expressed by the dimensionless constant called the equilibrium parameter, R_L, defined by

$$R_L = 1/(1 + K_L C_0) \quad (11)$$

where C_0 is the initial dye concentration (mg·L^{-1}).

R_L values indicate the type of isotherm to be irreversible (R_L = 0), favorable (0 < R_L < 1), linear (R_L = 1), or unfavorable (R_L > 1).[47] The R_L values for the adsorption of AG25, AB26, and AB7 on DS are shown in Table 3 for the single systems and Table 4 for the ternary systems.

An extended Langmuir model eq 12, was employed to fit the experimental data in the multicomponent system.[48]

Table 4. Isotherm Constants for Dye Adsorption by DS at Different Temperatures in Ternary System (200 mL Solution, pH 2, C_0 = 50 mg·L^{-1}, and DS = 2 g·L^{-1} for AG25, AB26, and AB7) (Q_0/mg·g^{-1}; K_L/L·mg^{-1}; K_F/L·g^{-1}; K_T/mg·L^{-1}; and B_1/mg·g^{-1})

	Extended Langmuir Isotherm Model											
	AG25				AB26				AB7			
temperature/°C	Q_0	K_L	R_L	R^2	Q_0	K_L	R_L	R^2	Q_0	K_L	R_L	R^2
25	36.101	0.162	0.109	0.999	39.682	0.336	0.056	0.999	33.333	0.105	0.160	0.999
35	36.363	0.177	0.102	0.999	39.682	0.403	0.047	0.999	33.670	0.110	0.153	0.999
45	36.630	0.193	0.094	0.999	39.682	0.499	0.038	0.999	34.130	0.116	0.147	0.999
55	36.764	0.214	0.085	0.999	39.526	0.649	0.029	0.999	34.483	0.123	0.140	0.999
65	36.900	0.239	0.077	0.999	39.370	0.904	0.022	0.998	34.843	0.131	0.132	0.999

	Extended Freundlich Isotherm Model											
	AG25				AB26				AB7			
	a_{12}	R^2	a_{13}	R^2	a_{21}	R^2	a_{23}	R^2	a_{31}	R^2	a_{32}	R^2
25	0.005	0.784	0.007	0.650	0.012	0.746	0.011	0.804	0.004	0.713	0.004	0.635
35	0.006	0.769	0.008	0.627	0.015	0.709	0.014	0.770	0.004	0.701	0.005	0.618
45	0.006	0.744	0.008	0.594	0.019	0.662	0.018	0.727	0.005	0.688	0.005	0.600
55	0.007	0.732	0.010	0.574	0.028	0.595	0.026	0.663	0.005	0.671	0.006	0.579
65	0.008	0.710	0.011	0.544	0.062	0.487	0.058	0.556	0.005	0.658	0.006	0.561

	Tempkin Isotherm Model								
	AG25			AB26			AB7		
	K_T	B_1	R^2	K_T	B_1	R^2	K_T	B_1	R^2
25	1.630	7.732	0.990	4.108	7.817	0.987	1.017	7.592	0.996
35	1.835	7.673	0.991	5.412	7.487	0.990	1.065	7.379	0.998
45	2.096	7.591	0.993	8.155	7.067	0.993	1.145	7.403	0.998
55	2.435	7.482	0.994	12.176	6.845	0.987	1.240	7.415	0.999
65	2.664	7.161	0.993	16.788	5.974	0.995	1.353	7.412	0.999

$$q_{e,i} = (K_{L,i}Q_{0,i}C_{e,i})/(1 + \sum K_{L,i}C_{e,i}) \quad (12)$$

where $K_{L,i}$ is the adsorption equilibrium constant of dye i in the mixed dye system.

In adsorption from ternary dye solutions, the amounts of dye adsorbed were expressed as

$$q_{e,1} = (K_{L,1}Q_{0,1}C_{e,1})/(1 + K_{L,1}C_{e,1} + K_{L,2}C_{e,2} + K_{L,3}C_{e,3}) \quad (13\text{-}1)$$

$$q_{e,2} = (K_{L,2}Q_{0,2}C_{e,2})/(1 + K_{L,1}C_{e,1} + K_{L,2}C_{e,2} + K_{L,3}C_{e,3}) \quad (13\text{-}2)$$

$$q_{e,3} = (K_{L,3}Q_{0,3}C_{e,3})/(1 + K_{L,1}C_{e,1} + K_{L,2}C_{e,2} + K_{L,3}C_{e,3}) \quad (13\text{-}3)$$

According to eq 13-1 to 13-3, we have

$$(K_{L,2}C_{e,2})/(K_{L,1}Q_{0,1}) = (q_{e,2}C_{e,2})/(q_{e,1}Q_{0,2}) \quad (14\text{-}1)$$

$$(K_{L,3}C_{e,3})/(K_{L,1}Q_{0,1}) = (q_{e,3}C_{e,1})/(q_{e,1}Q_{0,3}) \quad (14\text{-}2)$$

$$(K_{L,2}C_{e,2})/(K_{L,3}Q_{0,3}) = (q_{e,2}C_{e,3})/(q_{e,3}Q_{0,2}) \quad (14\text{-}3)$$

After rearrangement, a linear form of the extended Langmuir model in the ternary dye system was obtained.

$$(C_{e,1}/q_{e,1}) = (1/K_{L,1}Q_{0,1}) + (C_{e,1}/Q_{0,1}) + (q_{e,2}C_{e,1}/q_{e,1}Q_{0,2}) + (q_{e,3}C_{e,1}/q_{e,1}Q_{0,3}) \quad (15\text{-}1)$$

$$(C_{e,2}/q_{e,2}) = (1/K_{L,2}Q_{0,2}) + (C_{e,2}/Q_{0,2}) + (q_{e,1}C_{e,2}/q_{e,2}Q_{0,1}) + (q_{e,3}C_{e,2}/q_{e,2}Q_{0,3}) \quad (15\text{-}2)$$

$$(C_{e,3}/q_{e,3}) = (1/K_{L,3}Q_{0,3}) + (C_{e,3}/Q_{0,3}) + (q_{e,1}C_{e,3}/q_{e,3}Q_{0,1}) + (q_{e,2}C_{e,3}/q_{e,3}Q_{0,2}) \quad (15\text{-}3)$$

According to eq 15-1, the values of $C_{e,1}/q_{e,1}$ have a linear correlation with $C_{e,1}$ and $(q_{e,2}C_{e,1}/q_{e,1}Q_{0,2})$ and $(q_{e,3}C_{e,1}/q_{e,1}Q_{0,3})$ if the adsorption obeyed the extended Langmuir model. By using eq 15 as the fitting model, the isotherm parameters of an individual dye in the ternary dye solutions were estimated and are listed in Table 4. It can be seen that the isotherms of an individual dye in the ternary dye systems followed the extended Langmuir model.

The Freundlich isotherm is derived by assuming a heterogeneous surface with a nonuniform distribution of heat of adsorption over the surface. The Freundlich isotherm can be expressed by:[44−46,49]

$$q_e = K_F C_e^{1/n} \quad (16)$$

where K_F is the adsorption capacity at unit concentration and $1/n$ is adsorption intensity. The $1/n$ values indicate the type of isotherm to be irreversible ($1/n = 0$), favorable ($0 < 1/n < 1$), or unfavorable ($1/n > 1$).[46] Equation 16 can be rearranged to a linear form:

$$\log q_e = \log K_F + (1/n)\log C_e \quad (17)$$

The K_F and $1/n$ values for the Freundlich adsorption isotherm are shown in Table 3.

The Sheindrof−Rebhun−Sheintuch (SRS) equation is a multicomponent Freundlich-type equation and was based on the

assumption that there is an exponential distribution of adsorption energies available for each solute. A general form of the SRS equation may be written as

$$(q_e)_i^{j,k} = K_{Fi}C_{ei}\left(\sum (a_{ij}C_{ej} + a_{ik}C_{ek}\right)^{[(1/ni)-1]} \quad (18)$$

where $(q_e)_i^{j,k}$ is the amount of solute i adsorbed per unit weight of adsorbent in the presence of solute j and k. K_{Fi} is the single component Freundlich constant for solute i. $1/ni$ is the Freundlich exponential term for solute i. C_{ei}, C_{ej}, and C_{ek} are the equilibrium concentrations of solute i, j, and k, respectively, and a_{ij} and a_{ik} are the competitive coefficients.

The general SRS equation for a binary solute system can be written in the following form.

$$(q_e)_i^{j,k} = K_{Fi}C_{ei}(C_{ej} + a_{ij}C_{ej} + a_{ik}C_{ek})^{[(1/ni)-1]} \quad (19)$$

The linearized form of the equation is convenient to construct a competitive adsorption isotherm that measures the amount of solute adsorbed in the presence of competing solutes. To represent the batch isotherm data, the following linear forms of the SRS equation for a ternary solute system are used.

$$B_i = (C_{ei} + a_{ij}C_{ej} + a_{ik}C_{ek}) \quad (20)$$

where $B_i = [(q_e)_l^{j,k}/K_{Fi}C_{ei}]^{[ni/ni-1]}$ and a_{ji} and a_{ik} are the competitive coefficients for ternary systems. Competitive coefficients for ternary solute systems are computed by plotting B_i versus C_{ej} and C_{ek}.[50] The values of the competitive coefficients are listed in Table 4.

The Tempkin isotherm is given as:

$$q_e = RT/b \ln(K_T C_e) \quad (21)$$

which can be linearized as:

$$q_e = B_1 \ln K_T + B_1 \ln C_e \quad (22)$$

where

$$B_1 = RT/b \quad (23)$$

A plot of q_e versus ln C_e enables the determination of the isotherm constants B_1 (mg·g^{-1}) and K_T (mg·L^{-1}) from the slope and the intercept, respectively (Table 3 for the single system and Table 4 for the ternary system). K_T is the equilibrium binding constant corresponding to the maximum binding energy. The R and T are the gas constant (8.314 J·mol^{-1} K^{-1}) and the absolute temperature (K), respectively. The constant b is related to the heat of adsorption.

The Tempkin isotherm contains a factor that explicitly takes into account the adsorbing species adsorbent interactions. This isotherm assumes that (i) the heat of adsorption of all the molecules in the layer decreases linearly with coverage because of adsorbent−adsorbate interactions and (ii) the adsorption is characterized by a uniform distribution of binding energies, up to some maximum binding energy.[51,52]

The calculated coefficient of determination (R^2) shows that the dye removal isotherm using DS does not follow the Freundlich and Tempkin isotherms (Tables 3 and 4). The linear fit between the C_e/q_e versus C_e and the calculated coefficient of determination (R^2) for the Langmuir isotherm model show that the dye removal isotherm can be approximated as the Langmuir and the extended Langmuir isotherm models in single and ternary systems, respectively (Tables 3 and 4). This means that the adsorption of dyes takes place at specific homogeneous sites

Table 5. Thermodynamic Parameters of Dye Adsorption on DS in Single and Ternary Systems (200 mL solution, pH 2.5, and DS = 2 g·L^{-1} for AG25, AB26, and AB7) (Dye/mg·L^{-1}; ΔH^0/kJ·mol^{-1}; ΔS^0/J·mol^{-1}·K^{-1}; ΔG^0/kJ·mol^{-1})

				ΔG^0				
	dye	ΔH^0	ΔS^0	298 K	308 K	318 K	328 K	338 K
Single System					AG25			
	25	15.251	65.410	−4.241	−4.895	−5.549	−6.203	−6.857
	50	7.967	35.963	−2.750	−3.110	−3.469	−3.829	−4.188
	75	4.882	20.158	−1.125	−1.327	−1.528	−1.730	−1.932
					AB26			
	25	43.005	167.070	−6.782	−8.452	−10.123	−11.794	−13.465
	50	27.345	108.772	−5.069	−6.157	−7.245	−8.332	−9.420
	75	8.604	38.801	−2.958	−3.346	−3.734	−4.122	−4.510
					AB7			
	25	8.604	38.801	−2.958	−3.346	−3.734	−4.122	−4.510
	50	5.237	22.285	−1.403	−1.626	−1.850	−2.072	−2.295
	75	3.987	13.851	−0.141	−0.279	−0.418	−0.556	−0.695
Ternary System					AG25			
	25	10.328	65.410	−9.165	−9.819	−10.473	−11.127	−11.781
	50	6.583	46.118	−7.160	−7.621	−8.082	−8.543	−9.004
	75	4.592	18.302	−0.862	−1.045	−1.228	−1.411	−1.594
					AB26			
	25	33.321	129.299	−5.210	−6.503	−7.796	−9.089	−10.382
	50	15.251	65.410	−4.241	−4.895	−5.549	−6.203	−6.857
	75	6.976	31.350	−2.367	−2.680	−2.994	−3.307	−3.621
					AB7			
	25	6.583	29.438	−2.189	−2.484	−2.778	−3.072	−3.367
	50	4.730	19.200	−0.992	−1.184	−1.376	−1.568	−1.760
	75	3.786	12.060	0.192	0.072	−0.049	−0.170	−0.290

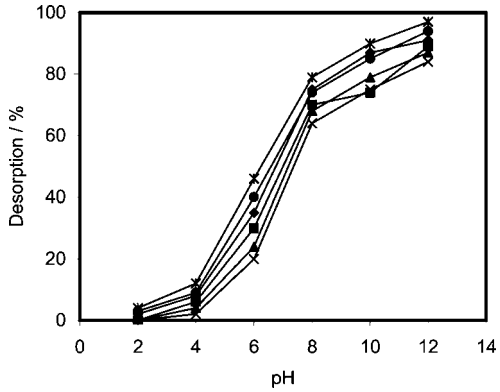

Figure 9. Effect of pH on the desorption of dyes from DS in single and ternary systems (pH 2, 25 °C, and DS = 2 g·L^{-1} for AG25, AB26, and AB7). ◆, AG25 (sin); ■, AG25 (ter); ▲, AB26 (sin); ×, AB26 (ter); ∗, AB7 (sin); and ●, AB7 (ter).

and one layer adsorption onto the DS surface in single and ternary systems.

Thermodynamic Studies. The thermodynamic parameters such as the change in Gibbs energy (ΔG), enthalpy (ΔH), and entropy (ΔS) were determined by using the following equations:

$$\Delta G = \Delta H - T\Delta S \tag{24}$$

$$K_c = C_A/C_S \tag{25}$$

$$\ln K_c = (\Delta S/R) - (\Delta H/RT) \tag{26}$$

where K_c, C_A, and C_S are the equilibrium constant, the amount of dye adsorbed on the adsorbent of the solution at equilibrium (mol·L^{-1}), and the equilibrium concentration of dye in the solution (mol·L^{-1}), respectively.

By plotting a graph of ln K_c versus 1/T, the values ΔH and ΔS can be estimated from the slopes and intercepts, respectively. Table 5 shows (the negative values of ΔG and positive ΔH) that the AG25, AB26, and AB7 dye adsorption onto DS is spontaneous and endothermic in the single and ternary systems. The positive value of ΔS suggests increased randomness at the solid−solution interface occurs in the internal structure of the adsorption of AG25, AB26, and AB7 dyes onto DS. The positive values of ΔH indicate the presence of an energy barrier in the adsorption process and an endothermic process.[53] The change in Gibbs energy for physisorption is between (−20 and 0) kJ·mol^{-1}, but chemisorption is in a range of (−80 to −400) kJ·mol^{-1}.[54] The values of ΔG obtained in this study are within the ranges of (−20 and 0) kJ·mol^{-1}, indicating that physisorption is the dominating mechanism.

Desorption Studies. Desorption studies help to elucidate the mechanism and recovery of the adsorbate and adsorbent. Desorption tests show that a maximum dye release of 91 % for AG25, 87 % for AB26, and 97 % for AB7 were achieved in aqueous solution at pH 12 (Figure 9). As the pH of the system increases, the number of negatively charged sites increased. A negatively charged site on the adsorbent favors desorption of the dye anions due to electrostatic repulsion. At pH 12, a significantly high electrostatic repulsion exists between the negatively charged surface of the adsorbent and the anionic dyes.

Conclusions

Kinetic, equilibrium, and thermodynamic studies were conducted for the adsorption of acid black 26 (AB26), acid green 25 (AG25), and acid blue 7 (AB7) from aqueous solutions onto DS in single and ternary systems. The results of adsorption showed that DS can be effectively used as a biosorbent for the removal of anionic dyes. The DS biosorbent exhibited high sorption capacities toward AG25, AB26, and AB7. The kinetic studies of dyes on DS were performed based on pseudofirst-order, pseudosecond-order, and intraparticle diffusion rate mechanisms. The data indicated that the adsorption kinetics of dyes on DS followed the pseudosecond-order model at different dye concentrations. The equilibrium data were analyzed using the Langmuir, Freundlich, and Tempkin isotherms, and the characteristic parameters for each isotherm were determined. The results showed that the experimental data were correlated reasonably well by the Langmuir and the extended Langmuir isotherm models in single and ternary systems, respectively. Thermodynamic studies indicated the presence of an energy barrier in the adsorption process and an endothermic process. Desorption studies were conducted, and the results showed that at alkaline pH values high electrostatic repulsion existed between the negatively charged surface of the adsorbent and the anionic dyes. On the basis of the data of the present study, one could conclude that the DS is an eco-friendly adsorbent for dye removal from colored textile wastewater.

Literature Cited

(1) Mahmoodi, N. M.; Arami, M. Immobilized titania nanophotocatalysis: Degradation, modeling and toxicity reduction of agricultural pollutants. *J. Alloys Compd.* **2010**, *506*, 155–159.
(2) Mahmoodi, N. M.; Arami, M. Degradation and toxicity reduction of textile wastewater using immobilized titania nanophotocatalysis. *J. Photochem. Photobiol., B* **2009**, *94*, 20–24.
(3) Mahmoodi, N. M.; Arami, M. Numerical finite volume modeling of dye decolorization using immobilized titania nanophotocatalysis. *Chem. Eng. J.* **2009**, *146*, 189–193.
(4) Mahmoodi, N. M.; Arami, M. Modeling and sensitivity analysis of dyes adsorption onto natural adsorbent from colored textile wastewater. *J. Appl. Polym. Sci.* **2008**, *109*, 4043–4048.
(5) Mahmoodi, N. M.; Arami, M. Bulk phase degradation of acid Red 14 by nanophotocatalysis using immobilized titanium (IV) oxide nanoparticles. *J. Photochem. Photobiol., A* **2006**, *182*, 60–66.
(6) Crini, G.; Badot, P. M. Application of chitosan, a natural aminopolysaccharide, for dye removal from aqueous solutions by adsorption processes using batch studies: A review of recent literature. *Prog. Polym. Sci.* **2008**, *33*, 399–447.
(7) Ramakrishna, K. R.; Viraraghavan, T. Dye removal using low cost adsorbents. *Water Sci. Technol.* **1997**, *36*, 189–196.
(8) Garg, V. K.; Kumar, R.; Gupta, R. Removal of malachite green dye from aqueous solution by adsorption using agro-industry waste: a case study of *Prosopis cineraria*. *Dyes Pigm.* **2004**, *62*, 1–10.
(9) Sanghi, R.; Bhattacharya, B. Review on decolorisation of aqueous dye solutions by low cost adsorbents. *Color. Technol.* **2002**, *118*, 256–269.
(10) Malik, P. K. Use of activated carbons prepared from sawdust and rice−husk for adsorption of acid dyes: a case study of Acid Yellow 36. *Dyes Pigm.* **2003**, *56*, 239–249.
(11) Stephenson, R. J.; Sheldon, J. B. Coagulation and precipitation of a mechanical pulping effluent. 1. Removal of carbon and turbidity. *Water Res.* **1996**, *30*, 781–792.
(12) Salem, I. A.; Elemaazawi, M. Kinetics and mechanism of color removal of methylene blue with hydrogen peroxide catalysed by some supported alumina surfaces. *Chemosphere* **2000**, *41*, 1173–1180.
(13) Crini, G.; Robert, C.; Gimbert, F.; Martel, B.; Adam, O.; De Giorgi, F. The removal of Basic Blue 3 from aqueous solutions by chitosan-based adsorbent: batch studies. *J. Hazard. Mater.* **2008**, *153*, 96–106.
(14) Dutta, P. K.; Bhavani, K. D.; Sharma, N. Adsorption for dyehouse effluent by low cost adsorbent (chitosan). *Asian Textile J.* **2001**, *10*, 57–63.
(15) Rao, N. N.; Somasekhar, K. M.; Kaul, S. N.; Szpyrkowicz, L. Electrochemical oxidation of tannery waste water. *J. Chem. Technol. Biotechnol.* **2001**, *76*, 1124–1131.
(16) Meshko, V.; Markovska, L.; Mincheva, M.; Rodrigues, A. E. Adsorption of basic dyes on granular activated carbon and natural zeolite. *Water Res.* **2001**, *35*, 3357–3366.
(17) Kannan, N.; Sundaram, M. M. Kinetics and mechanism of removal of methylene blue by adsorption on various carbons—a comparative study. *Dyes Pigm.* **2001**, *51*, 25–40.

(18) Annadurai, G.; Juang, R. S.; Lee, D. J. Factorial design analysis for adsorption of dye on activated carbon beads incorporated with calcium alginate. *Adv. Environ. Res.* **2002**, *6*, 191–198.
(19) EL-Geundi, M. S. Adsorbents for industrial pollution control. *Adsorpt. Sci. Technol.* **1997**, *15*, 777–787.
(20) Mall, I. D.; Srivastava, V. C.; Agarwal, N. K.; Mishra, I. M. Removal of congo red from aqueous solution by bagasse fly ash and activated carbon: kinetic study and equilibrium isotherm analyses. *Chemosphere* **2005**, *61*, 492–501.
(21) El Mouzdahir, Y.; Elmchaouri, A.; Mahboub, R.; Gil, A.; Korili, S. A. Adsorption of Methylene Blue from Aqueous Solutions on a Moroccan Clay. *J. Chem. Eng. Data* **2007**, *52*, 1621–1625.
(22) Selim, Y.; Hasdemir, M. Removal of Some Carboxylic Acids from Aqueous Solutions by Hydrogels. *J. Chem. Eng. Data* **2008**, *53*, 2351–2355.
(23) Al-Muhtaseb, S. A. Adsorption and Desorption Equilibria of Nitrogen, Methane, Ethane, and Ethylene on Date-Pit Activated Carbon. *J. Chem. Eng. Data* **2010**, *55*, 313–319.
(24) Bouchelta, C.; Medjram, M. S.; Bertrand, O.; Bellat, J. P. Preparation and characterization of activated carbon from date stones by physical activation with steam. *J. Anal. Appl. Pyrolysis* **2008**, *82*, 70–77.
(25) Barreveld, W. H. *Date Palm Products*, FAO Agricultural Services, Bulletin no. 101; Food and Agriculture Organization of the United Nations: Rome, Italy, 1993.
(26) Zollinger, H. *Color chemistry: syntheses, properties and applications of organic dyes and pigments*, 2nd ed.; VCH Verlagsgesllschaft mbH: Weinheim, Germany, 1991.
(27) Pavia, D. L.; Lampman, G. M.; Kaiz, G. S. *Introduction to Spectroscopy: A Guide for Students of Organic Chemistry*; W.B. Saunders Company: Philadelphia, PA, 1987.
(28) Chiou, M. S.; Li, H. Y. Adsorption behavior of reactive dye in aqueous solution on chemical cross-linked chitosan beads. *Chemosphere* **2003**, *50*, 1095–1105.
(29) Chatterjee, S.; Chatterjee, S.; Chatterjee, B. P.; Das, A. R.; Guha, A. K. Adsorption of a model anionic dye, eosin Y, from aqueous solution by chitosan hydrobeads. *J. Colloid Interface Sci.* **2005**, *288*, 30–35.
(30) Namasivayam, C.; Kavitha, D. Removal of Congo Red from water by adsorption onto activated carbon prepared from coir pith, an agricultural solid waste. *Dyes Pigm.* **2002**, *54*, 47–58.
(31) Alkan, M.; Dogan, M. Adsorption kinetics of Victoria blue onto perlite. *Fresenius Environ. Bull.* **2003**, *12*, 418–425.
(32) Asfour, H. M.; Fadali, O. A.; Nassar, M. M.; El-Geundi, M. S. Equilibrium studies on dsorption of basic dyes on hardwood. *J. Chem. Technol. Biotechnol.* **1985**, *35*, 21–27.
(33) Ho, Y. S. Adsorption of heavy metals from waste streams by peat. Ph.D. Thesis, The University of Birmingham, Birmingham, U.K., 1995.
(34) Lagergren. Zur theorie der sogenannten adsorption geloster stoffe. *K. Sven. Vetenskapsakad. Handl.* **1898**, *24*, 1–39.
(35) Ho, Y. S. Sorption studies of acid dye by mixed sorbents. *Adsorption* **2001**, *7*, 139–147.
(36) Ho, Y. S. Citation review of Lagergren kinetic rate equation on adsorption reactions. *Scientometrics* **2004**, *59*, 171–177.
(37) Ho, Y. S.; McKay, G. Pseudo-second order model for sorption processes. *Process Biochem.* **1999**, *34*, 451–465.
(38) Ozcan, A.; Ozcan, A. S. Adsorption of Acid Red 57 from aqueous solutions onto surfactant-modified sepiolite. *J. Hazard. Mater.* **2005**, *125*, 252–259.
(39) Senthilkumaar, S.; Kalaamani, P.; Porkodi, K.; Varadarajan, P. R.; Subburaam, C. V. Adsorption of dissolved reactive red dye from aqueous phase onto activated carbon prepared from agricultural waste. *Bioresour. Technol.* **2006**, *97* (14), 1618–1625.
(40) Weber, W. J.; Morris, J. C. Kinetics of adsorption on carbon from solution. *J. Sanit. Eng. Div., Am. Soc. Civ. Eng.* **1963**, *89* (SA2), 31–60.
(41) Langmuir, I. The constitution and fundamental properties of solids and liquids. I. Solids. *J. Am. Chem. Soc.* **1916**, *38*, 2221–2295.
(42) Langmuir, I. The constitution and fundamental properties of solids and liquids. II. Liquids. *J. Am. Chem. Soc.* **1917**, *39*, 1848–1906.
(43) Langmuir, I. The adsorption of gases on plane surfaces of glass, mica and platinum. *J. Am. Chem. Soc.* **1918**, *40*, 1361–1403.
(44) Alley, E. R. *Water Quality Control Handbook*; McGraw-Hill Education: London, 2000; pp 125−141.
(45) Benefield, L. D.; Judkins, J. F.; Weand, B. L. *Process Chemistry for Water and Wastewater Treatment*; Prentice Hall: Englewood Cliffs, NJ, 1982; pp 191−210.
(46) Woodard, F. *Industrial Waste Treatment Handbook*; Butterworth-Heinemann: Boston, 2001; pp 376−451.
(47) Hall, K. R.; Eagleton, L. C.; Acrivos, A.; Vermeulen, T. Pore and solid diffusion kinetics in fixed-bed adsorption under constant pattern conditions. *Ind. Eng. Chem. Fundam.* **1966**, *5*, 212–223.
(48) Asku, Z.; Tezar, S. Biosorption of reactive dyes on the green alga *Chlorella vulgaris*. *Process Biochem.* **2006**, *40*, 1349.
(49) Freundlich, H. M. F. Uber die adsorption in lasugen. *Z. Phys. Chem.* **1906**, *57*, 385–470.
(50) Vinod, V. P.; Anirudha., T. S. Adsorption behavior of basic dyes on the humic acid immobilized pillared clay. *Water, Air, Soil Pollut.* **2003**, *150*, 193–217.
(51) Tempkin, M. J.; Pyzhev, V. Recent modification to Langmiur isotherms. *Acta Physiochim. USSR* **1940**, *12*, 217–222.
(52) Kim, Y. C.; Kim, I.; Choi Rengraj, S.; Yi, J. Arsenic removal using mesoporous alumina prepared via a templating method. *Environ. Sci. Technol.* **2004**, *38*, 924–31.
(53) Ozcan, A. S.; Ozcan, A. Adsorption of acid dyes from aqueous solutions onto acid-activated bentonite. *J. Colloid Interface Sci.* **2004**, *276*, 39–46.
(54) Jaycock, M. J.; Parfitt, G. D. *Chemistry of Interfaces*; Ellis Horwood Ltd.: Onichester, 1981.

Received for review March 13, 2010. Accepted September 24, 2010.

JE1002384